Transaction B: Mechanical Engineering
Vol. 17, No. 2, pp. 83–92

SCIENTIA IRANICA

Three-Dimensional Simulation of Turbulent Flow in 3-Sub Channels of a VVER-1000 Reactor

H. Ganjiani[1] and B. Firoozabadi[2,*]

Abstract. *In this study, the fluid dynamics and convective heat transfer for turbulent flows through a 3-sub channel of a rod bundle, which is representative of those used in VVER-1000, are examined. The rod bundle is constructed from parallel rods in a hexagonal array. The rods are on constant pitch by spacer grids spaced axially along the rod bundle. The geometry details of the bundle and heat flux from the fuel rod are similar to that of the Iranian nuclear reactor under construction. A numerical study using Computational Fluid Dynamics (CFD) was carried out to estimate the flow field, pressure loss and heat transfer coefficients in spacer grids and rod bundles. Turbulence has been modeled using the $k-\varepsilon$ turbulence model. At a distance of $2D_h$ from the beginning of the spacer grids, in the direction of flow, because fluid enthalpy and Nusselt numbers have maximum and minimum values, respectively, the probability of nucleate boiling (PNB) is much higher, and a two phase flow will occur. Predicted results are found to be in close agreement with those of the experimental results reported in the literature.*

Keywords: *Sub channel; Rod bundle; Spacer grid; Computational Fluid Dynamics (CFD); Turbulent flow; Nusselt number.*

INTRODUCTION

The basic role of a reactor in a nuclear power plant is the generation of heat energy. This heat energy is generated from nuclear fission in fuel rods and the transfer to a liquid coolant that flows in the space between the rods. The rod bundle is constructed from parallel fuel rods.

A series of spacer grids spaced axially along the rod bundle provides structural support for the fuel rods. In addition to positioning the fuel rods, the spacer grids affect the hydrodynamics of the pressurized water and heat transfer from the rods. The spacer grids locally reduce the flow area through the rod bundle. This causes flow acceleration and deceleration in regions upstream and downstream of the spacer grid, respectively. The growth of the thermal and hydrodynamic boundary layer along the surfaces of the rods is disrupted by a spacer grid. In addition, the spacer grid increases the turbulence intensity in the flow just downstream of the spacer grid [1]. Spacer grids are different in reactors.

Rehme and Trippe [2] conducted some experiments on turbulent flows through rod bundles and analyzed their pressure drop. Detailed measurements of the velocity distributions in a hexagonal 19-rod bundle were compared with predictions for fully developed turbulent flows. Pressure drop correlations for fully developed flows, for both turbulent and laminar flows through rod bundles, were established by calculations based on theoretical studies. The frictional pressure losses were determined based on a function of the Reynolds number and geometry factors. Rehme and Trippe [2] outlines a method for determining the turbulent flow geometry factors based on the laminar flow geometry factor, which can be calculated for any geometry by solving Poisson's equation. The friction factors obtained agree well with experimental measurements over a variety of rod bundle geometry parameters. In addition, correlations for calculation of the pressure loss due to spacer grids were presented and compared with experimental data.

Sato et al. [3] reported a method for obtaining

1. *Department of Nuclear Engineering, Shahid Beheshti University, Evin, Tehran, P.O. Box 1983963113, Iran.*
2. *School of Mechanical Engineering, Sharif University of Technology, Tehran, P.O. Box 11155-9567, Iran.*
*. *Corresponding author. E-mail: firoozabadi@sharif.edu*

Received 23 December 2008; received in revised form 2 September 2009; accepted 16 January 2010

friction factors based on the geometry factor of the rod bundle sub channels. For P/D and W/D ratios of approximately 1.3, the geometry factor for a square array rod bundle is within 5% of the geometry factor for a turbulent flow in a smooth pipe. Thus, the friction factors are well predicted by the correlations developed for a turbulent flow in a smooth pipe.

Rehme [4] reviewed the published data in order to form a complete picture of the turbulent structure in rod bundle sub channels and the natural mixing between the interconnected sub channels. Rehme [4] concluded that the secondary flow velocities do not cause the high mixing rates observed in rod bundles with small gap sizes. Review of the measured Reynolds stress data highlighted that the eddy viscosities measured normal to the rod surface are comparable to data obtained from circular tubes and have only a small dependence on the relative gap size. However, the eddy viscosities parallel to the rod surfaces have a strong dependence on the gap size and increase as the gap size is decreased. Thus, the anisotropy of the eddy viscosities increases with a decreasing of the gap size. Rehme [4] concluded that the macroscopic flow pulsations across sub channel gaps are the reason for high mixing rates between sub channels. A comparison between the mixing factors determined based on experimental data and those determined based on the periodic flow pulsations are in good agreement, which supports the conclusion in rod bundles that the macroscopic flow pulsations cause the high mixing rates observed.

Rehme [5] carried out a systematic experimental study of turbulent flows through sub channels of a rectangular channel with four parallel rods. The data show that the structure of turbulent flows through the rod bundles is different from turbulent flows through circular tubes, at least for P/D and W/D ratios less than 1.2.

An investigation of spacer grids with mixing vanes affecting the turbulent structure in the sub channels of a 5×5 rod bundle were performed experimentally by Yang and Chung [6]. The detailed hydraulic characteristics were measured by using a Laser Doppler Velocimeter. For evaluating the friction factor for a rod bundle and the loss coefficient for the spacer grid, pressure drop measurements were also performed.

Imaizumi et al. [7] compared measurements and CFD estimation of pressure distribution near a spacer grid. Hoshi et al. [8], Teshima et al. [9] and In [10] carried out CFD analyses to estimate the coolant flow mixing downstream of spacer grids, which is created by deflectors on the spacer grid, and compared the velocity measurements.

Jian et al. [11] developed a simple analytical method for the prediction of the friction factor, f, of fully developed turbulent flows and the Nusselt number, Nu, of fully developed turbulent forced convection in rod bundles arranged in square or hexagonal arrays. The method was based on the law of the wall for velocity and the law of the wall for the temperature, which were integrated over the entire flow area to yield algebraic equations for the prediction of f and Nu. Jian et al. [11] derived an algebraic equation for the friction factor of turbulent flow in smooth rod bundles in a similar form to the classical equation for the friction factor of turbulent flow in a smooth circular tube. An explicit equation for the Nusselt number of turbulent forced convection in these rod bundles, as a function of the friction factor, Reynolds number and Prandtl number, was developed. Their method is applicable to infinite rod bundles in square and hexagonal arrays with a low pitch to rod diameter ratio, $P/D < 1.2$, extended the analysis to rod bundles with a rough surface and provided a method for the prediction of the friction factor and the Nusselt number.

Bottcher [12] carried out a CFD model for the complete VVER-1000 reactor pressure vessel. Due to computational limits, details of the core and some other geometry are not modeled. Detailed coolant flow in the rod bundle and sub channels was not investigated in his study.

Since excessive heat is generated in fuel rods, the investigation details of the flow field and heat transfer in sub channels are very important. Therefore, a numerical study using CFD under a single-phase flow condition was carried out to estimate the pressure loss, velocity and temperature distributions in a sub channels fuel rod bundle of a VVER-1000 reactor.

CFD MODELING

Geometry and Mesh

VVER-1000 is a pressurized water reactor with an open type of hexagonal core geometry that contains 163 fuel assemblies. The fuel assembly VVER-1000 reactor consists of 311 fuel rods of diameter 9.1 mm arranged in hexagonal arrangements (Figure 1), which is the same as that of the Iranian nuclear reactor under construction in Boshehr, Iran. The rod bundle investigation was conducted using an approximately 3.837-m long assembly of fourteen spans with fifteen spacer grids.

Due to the limitations in computer hardware resources, it is difficult to analyze the whole of the flow field in the rod bundle. Therefore, the first 700 mm length of a 3-rod bundle with two spacer grids was selected for the analysis.

The computational domain is shown in Figure 2. The structural model of a rod bundle with a spacer grid is shown in Figure 3; schematics of the rod and

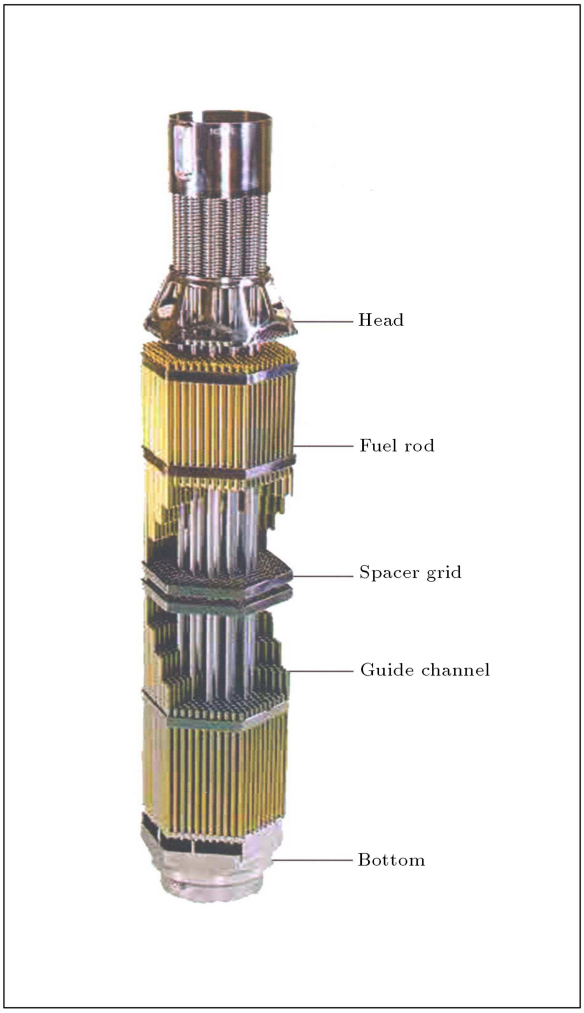

Figure 1. Fuel assembly for VVER-1000 reactor.

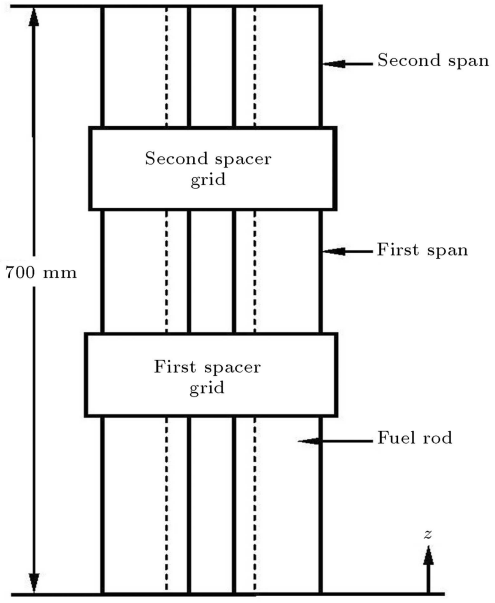

Figure 2. Computational domain.

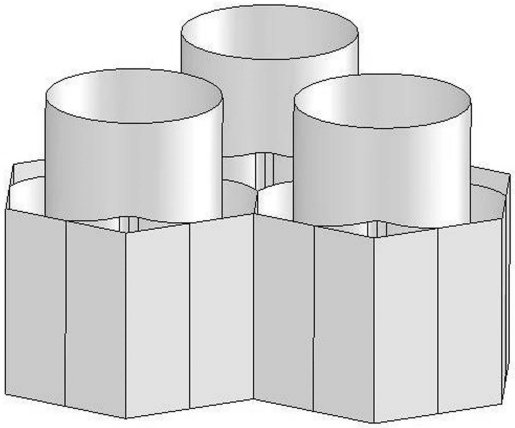

Figure 3. Rod bundle with a spacer grid model.

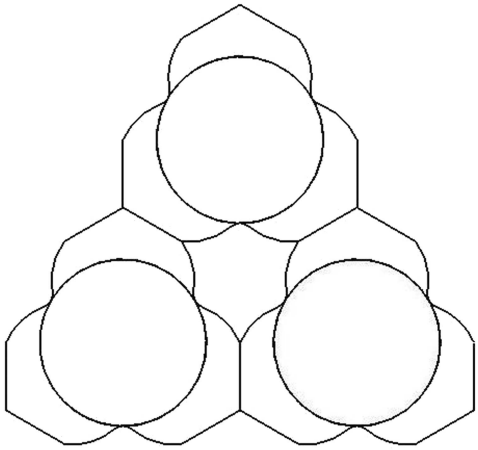

Figure 4. Rods and spacer grids arrangement (top view).

spacer grid arrangement are also shown in Figure 4. The first, the model of three rods and spacer grids, is created in CAD packages software. Then, the surface is exported to the CFD code and volumetric tetrahedral cells are created. The generated mesh is shown in Figure 5. The analysis was performed by an inhouse CFD code using the QUICK numerical scheme and two turbulence models, i.e. standard $k-\varepsilon$ and the standard Reynolds Stress Turbulence (RSM) model. The same results were achieved by these models, but since the standard $k-\varepsilon$ model showed a fairly fast convergence, the standard $k-\varepsilon$ model was selected in this study. All the simulations were conducted by means of a segregated method using the SIMPLE scheme [13] for pressure-velocity coupling. A total of 2,000,000 cells were created (which required a computer with at least a 2 GB RAM).

Governing Equations

The equations that govern the fluid flow and heat transfer process in the rod bundle are as follows [14]:

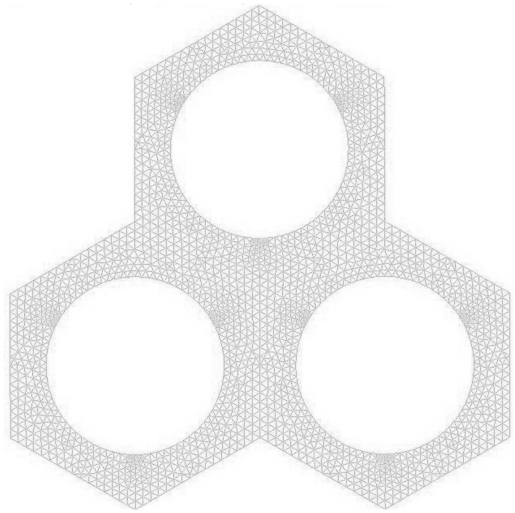

Figure 5. Mesh distribution in a cross sectional view.

- Continuity:

$$\frac{\partial}{\partial x_j}(\rho u_j) = 0. \tag{1}$$

- Momentum:

$$\frac{\partial}{\partial x_j}(\rho u_j u_i - \tau_{ij}) = -\frac{\partial p}{\partial x_i}, \tag{2}$$

where:

$$\tau_{ij} = 2\mu s_{ij} - \frac{2}{3}\mu\frac{\partial u_k}{\partial x_k}\delta_{ij} - \rho\bar{u}_i'\bar{u}_j', \tag{3}$$

and:

$$s_{ij} = \frac{1}{2}\left(\frac{\partial u_i}{\partial x_j} + \frac{\partial u_j}{\partial x_i}\right). \tag{4}$$

- Energy:

$$\frac{\partial}{\partial x_j}(\rho u_j c_p T - F_{h,j}) = 0, \tag{5}$$

where:

$$F_{h,j} = K\frac{\partial T}{\partial x_j} - \rho c_p \bar{u}_j'\bar{T}'. \tag{6}$$

The standard $k-\varepsilon$ model equations [15]:

- Turbulent kinetic energy:

$$\frac{\partial}{\partial x_j}\left[\rho u_j k - \left(\mu + \frac{\mu_t}{\sigma_k}\right)\frac{\partial k}{\partial x_j}\right] = -\rho\varepsilon - \frac{2}{3}\left(\mu_t\frac{\partial u_i}{\partial x_i} + \rho k\right)\frac{\partial u_i}{\partial x_i}. \tag{7}$$

- Turbulent dissipation rate:

$$\frac{\partial}{\partial x_j}\left[\rho u_j \varepsilon - \left(\mu + \frac{\mu_t}{\sigma_k}\right)\frac{\partial \varepsilon}{\partial x_j}\right] = -C_{\varepsilon 1}\frac{\varepsilon}{k}\left[-\frac{2}{3}\left(\mu_t\frac{\partial u_i}{\partial x_i} + \rho k\right)\frac{\partial u_i}{\partial x_i}\right] - C_{\varepsilon 2}\rho\frac{\varepsilon^2}{k}. \tag{8}$$

Boundary Conditions

The boundary conditions imposed on Equations 1 to 8 in sub channels are presented in Figure 6. The hydraulic diameter of the bundle is 5.2 mm. For the flow calculations, the solid surfaces of the fuel rod and spacer grid have no slip boundary condition, and a symmetric condition was imposed on the other outer surface. In the thermal study, the heat flux over the fuel rods is specified. The heat flux, 278.7 kW/m^2, specified over the surface of the rods, corresponds to the average value of the axial heat flux in modeling of the domain in the VVER-1000 reactor at full power (3000 MW) [16,17]. This method is expressed in the Appendix. The inlet velocity of water and the inlet water temperature are 5.6 m/s and 291°, respectively. The Reynolds number for this inlet velocity is 2.3×10^5 and is well inside the turbulent flow regime. The fluid flows upward in the fuel assembly.

RESULTS AND DISCUSSION

Velocity Distribution

The contours of the axial velocity at various axial planes along the flow direction after the first spacer grid are depicted in Figures 7a to 7d. Figure 8 shows variation axial bulk velocity after two spacer grids. It is observed that the axial flow after any spacer grid has a similar profile that differs by increments. Due to the complex flow present in rod bundle sub channels, which

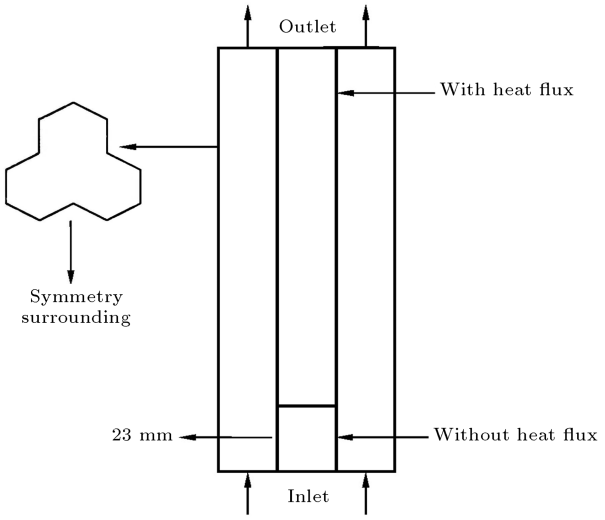

Figure 6. Boundary conditions.

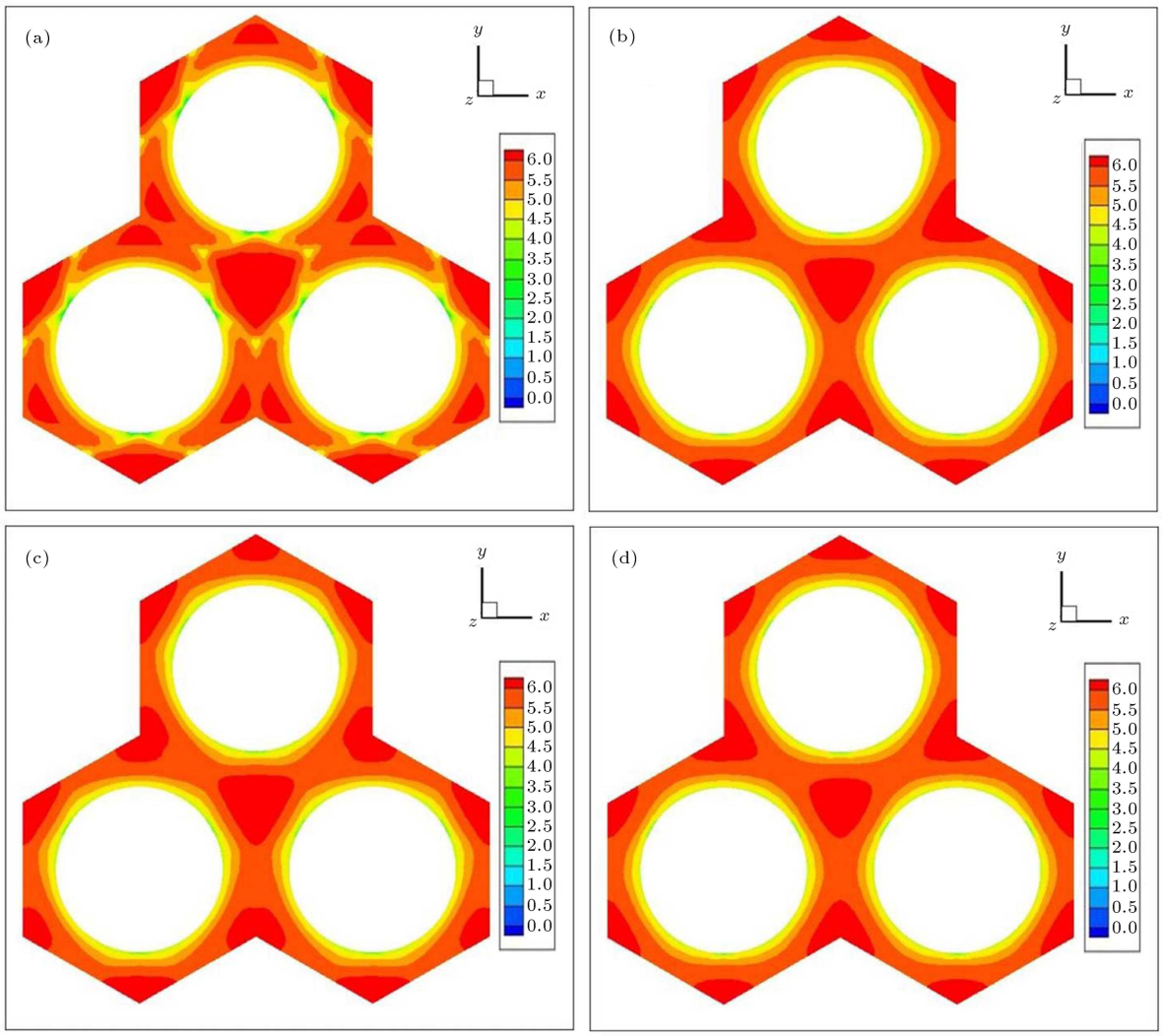

Figure 7. Axial velocity distribution, W (m/s): (a) $Z = 0D_h$, (b) $Z = 8D_h$, (c) $Z = 16D_h$ and (d) $Z = 32D_h$.

exhibit a secondary flow, mixing between sub channels and unsteady flow pulsations, true fully-developed flow conditions are not as directly achieved. The streamwise distance required to reach fully-developed flow conditions in a rod bundle sub channel varies from

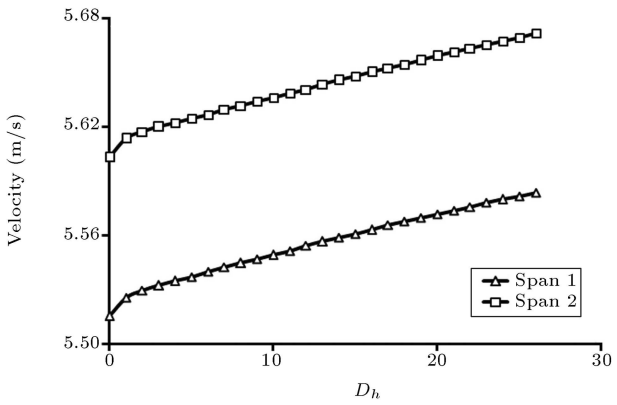

Figure 8. Development axial bulk velocity in 2 spans.

the number of rods in the bundle, the type of rod array and the rod bundle construction. For rod bundles constructed using a series of spacer grids, the axial spacing between the spacer grids can be long enough for fully-developed flow conditions to develop in the span between two consecutive spacer grids. The ratio of the maximum velocity to average velocity decreases from 1.18 to 1.15 at 25 hydraulic diameters, after any spacer grids, beyond which it changes very little. This also indicates that the flow has reached full development at 25 hydraulic diameters.

The secondary flow intensity is defined as the magnitude of the secondary flow vector divided by axial bulk mean velocity, as described in Equation 9:

$$VI_{\text{cross}} = \frac{1}{A} \int \left(\frac{\sqrt{U_1^2 + U_2^2}}{U_{\text{bulk}}} \right) dA, \tag{9}$$

where U_{bulk} is the axial bulk velocity.

Lee et al. [18] showed that the secondary flow,

even if its magnitude is small, is important because it greatly influences the promotion of heat transfer from rods to sub channels and affects the mean axial velocity, turbulent kinetic energy and wall shear stress distributions. Figure 9 shows the development of secondary flow intensities, VI_{cross}, after two spacer grids.

VI_{cross} shows an abrupt increase in secondary flow intensities just after the spacer grids, but a subsequent rapid decrease as the flow goes downstream.

Pressure Drops

Figure 10 shows the development of pressure drops in the axial direction. As shown in Figure 10, the behavior of the pressure drop in the rod bundle between the spacer grids is linear and, when across, the spacer grids deviated from linearity and increased the pressure drops.

Typically, the pressure drop across a spacer grid is expressed using a pressure loss coefficient. The pressure drop at the spacer grid is expressed as:

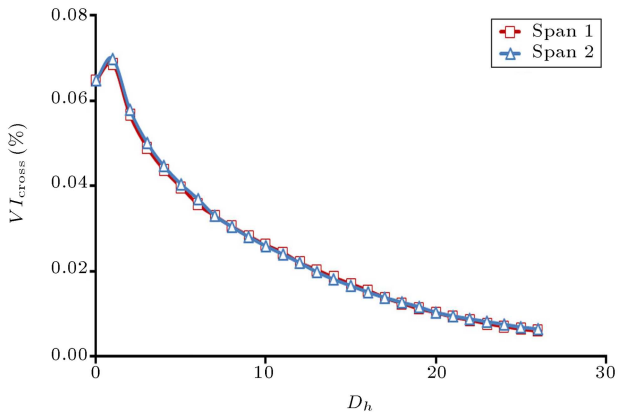

Figure 9. Developments of cross-sectional velocity intensities.

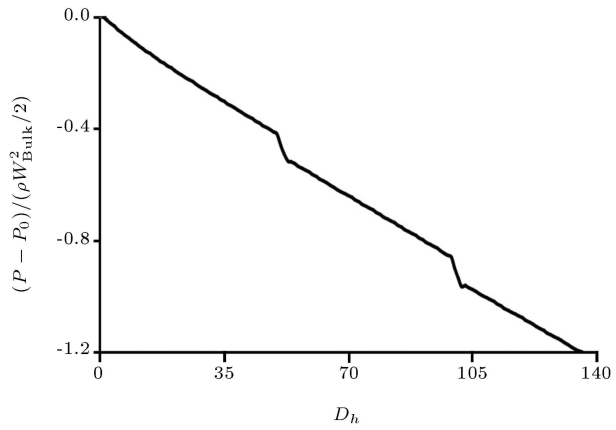

Figure 10. Developments of pressure drops.

$$\Delta P_{sg} = \frac{C_B \rho U^2_{\text{bulk}}}{2}, \tag{10}$$

where C_B is the loss coefficient of the spacer grid.

Rehme [19] proposed a correlation for the loss coefficient of a spacer grid based on the blockage ratio of the spacer grid:

$$C_B = C\varepsilon_g^2, \tag{11}$$

where ε_g is the blockage ratio of the spacer grid and is defined as the ratio of the projected area of the spacer grid to the open flow area through the rod bundle:

$$\varepsilon_g = \frac{A_{sg}}{A_{rb}}. \tag{12}$$

For a Reynolds number greater than 5×10^4, the value of C in Equation 11 is between 6 and 7. In Table 1, the pressure loss coefficients are compared with the Rehme's data [19]. The present result is in a reasonable range compared with this data [19].

Friction factor, f, was evaluated to analyze the friction loss in the rod bundle, i.e.:

$$f = \frac{\Delta P_{rb}}{0.5\rho U^2_{\text{bulk}}} \frac{D_h}{L}. \tag{13}$$

In general, the rods and walls of the rod bundle are smooth, and the friction factors are compared with the friction factors established for turbulent flow in a smooth pipe as obtained from the Moody diagram or alternative correlation, such as the correlation proposed by Prandtl [20]:

$$\frac{1}{\sqrt{f}} = 2.0 \log_{10}\left(\text{Re}_{D_h}\sqrt{f}\right) - 0.8. \tag{14}$$

For a rod bundle of finite dimensions, the hydraulic diameter of the rod bundle, D_h, is the appropriate characteristic length to use for calculation of the friction factor. The friction factor is compared with the Moody's correlation for a smooth tube [21], Yang and Chung's data [22] and the Prandtl correlation in Figures 11 and 12, respectively. The results show that the friction factors for rod bundle are lower than the values given in the Moody's charts. The reason is not clear because, in general, the difference of configuration between the rod bundle and circular tube and, moreover, the friction factors for rod bundles depends on various kinds of geometric parameters, such as P/D and the type of spacer grid [23].

Table 1. Comparison of the pressure loss coefficient of spacer grids.

Rehme [19]	Present Study
0.0936	0.0913

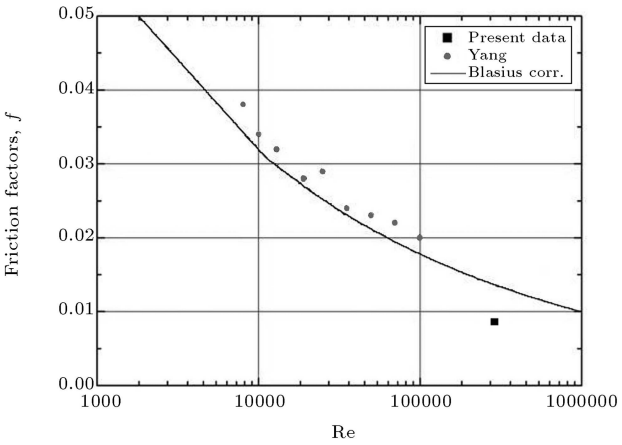

Figure 11. Comparison of the friction factor with Blasius correlation and Yang's data.

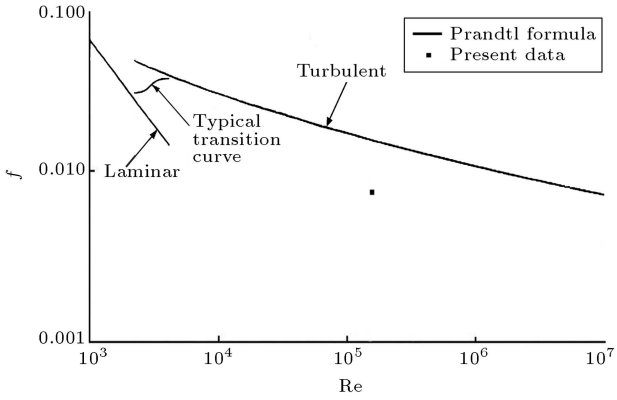

Figure 12. Comparison of the friction factor with Prandtl correlation.

Temperature Distribution

The water temperature development along the axial direction after the first spacer grid is presented in Figures 13a to 13d in the form of contours. To evaluate the heat transfer characteristics directly, the non-dimensional Nusselt number, Nu, is used. Nu is defined by Equation 15:

$$\mathrm{Nu} = \frac{hD_h}{k}. \tag{15}$$

The Dittus-Boetlter equation [24];

$$\mathrm{Nu} = 0.023\mathrm{Re}^{0.8}\mathrm{Pr}^{0.4}, \tag{16}$$

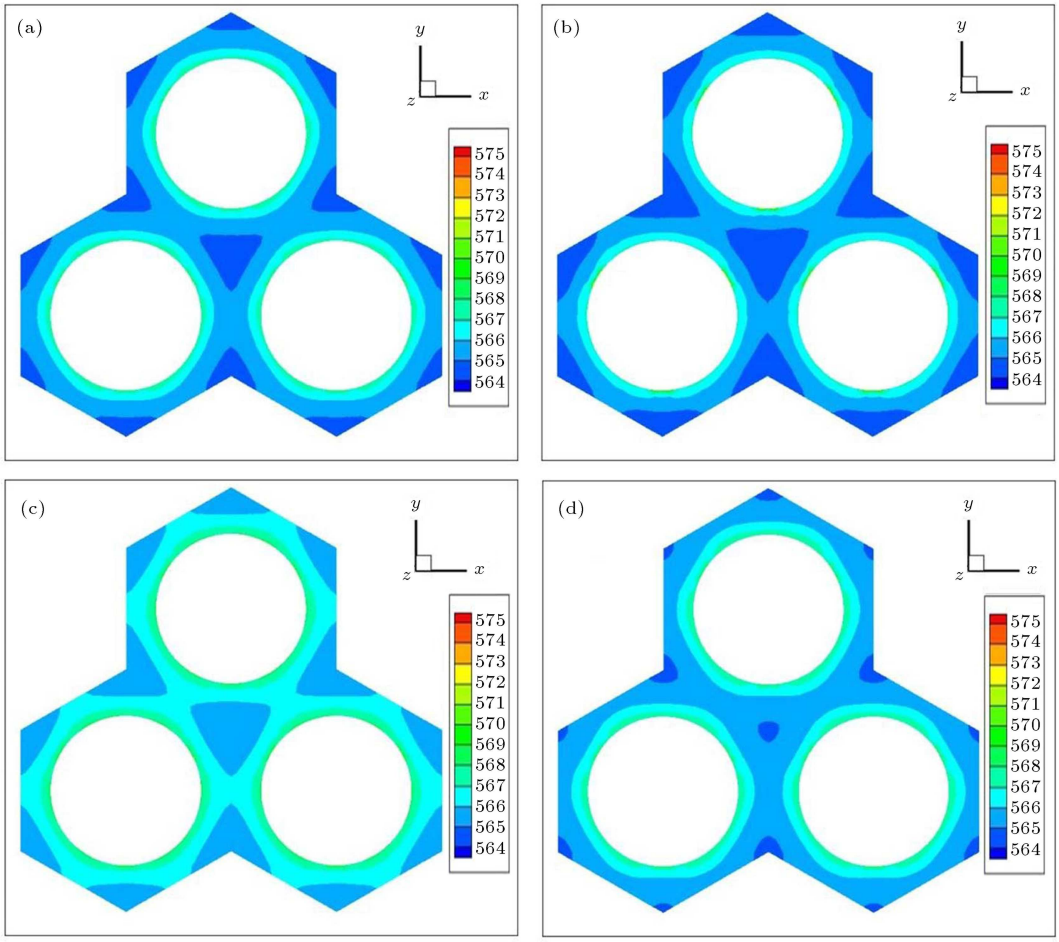

Figure 13. Axial temperature distribution: (a) $Z = 0D_h$, (b) $Z = 8D_h$, (c) $Z = 16D_h$ and (d) $Z = 32D_h$.

is the basic correlation developed hydrodynamically and thermally for fully-developed pipe flows that have been used as benchmarks for measurements of fully-developed heat transfer coefficients in rod bundles.

Yao et al. [25] developed a correlation for the axial developed flow of heat transfer downstream of spacer grids, based on the flow blockage of the spacer grid:

$$\frac{\mathrm{Nu}}{\mathrm{Nu}_{fd}} = 1 + 5.55\varepsilon_g^2 e^{-0.13\frac{Z}{D_h}}, \qquad (17)$$

where ε_g is the blockage ratio of the spacer grid.

The normalized Nusselt numbers decrease with increasing axial distance downstream of the spacer grid. In Figure 14, the ratio, $\mathrm{Nu}/\mathrm{Nu}_{fd}$, was compared with Yao's correlation. At an axial location of $25D_h$, the heat transfer enhancement has decayed to approximately 1, which indicates fully-developed flow conditions at spans. The difference between normalized Nusselt numbers is obtained in this study, and Yao's correlation at this location is 26.8%. Figure 14 shows the abrupt increase in normalized Nussselt number just after the spacer grid due to the action of the secondary flow.

Developments of fluid enthalpy and Nussselt number in the computational domain are shown in Figures 15 and 16, respectively. At a distance of $2D_h$ from the beginning of the spacer grids, in the direction of the flow, fluid enthalpy has maximum values (peaks in Figure 15) and the Nusselt number has minimum values (bottoms in Figure 16). In this place, because fluid enthalpy and Nusselt number have maximum and minimum values, respectively, the probability of nucleate boiling (DNB) is much higher, and two phase flow will occur.

Although the DNB phenomenon is analyzed by CFD under a two phase flow, the distribution of fluid enthalpy and Nusselt number under a single phase flow will determine initial conditions and important information regarding the two phase flow structure.

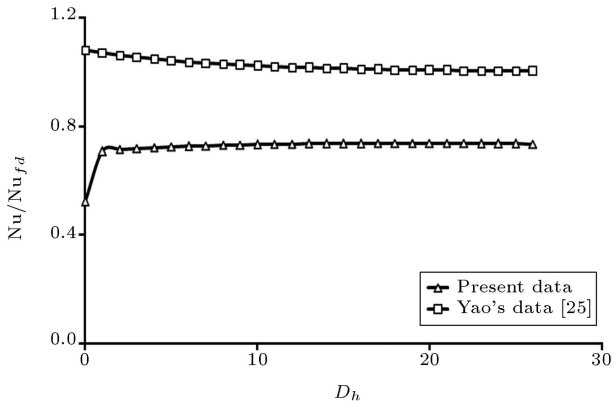

Figure 14. Developments of normalized Nusselt numbers.

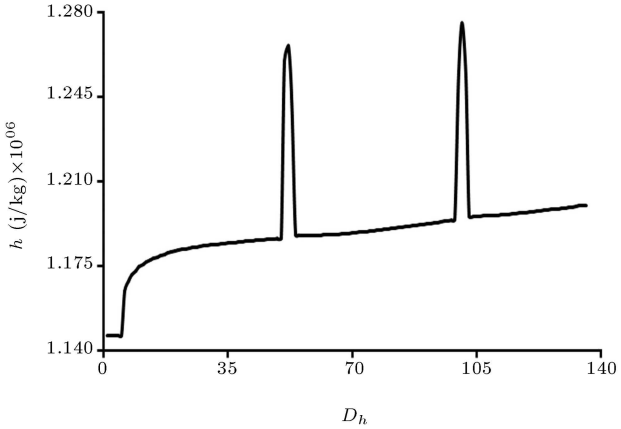

Figure 15. Developments of fluid enthalpy.

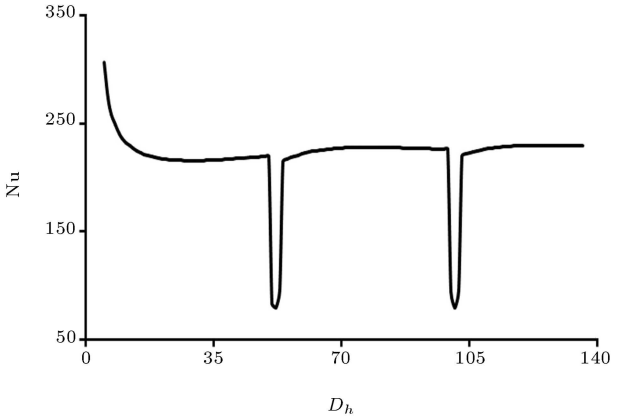

Figure 16. Developments of Nusselt number.

CONCLUSION

A three-dimensional computational fluid dynamic analysis of turbulent flows around 3 rods with spacer grids is carried out. The profile of the flow in the spans is similar and the spacer grids create a small amount of secondary flow in the sub channels that decay rapidly.

The spacer grids increase pressure drop and the value of the coefficient pressure loss of spacer grids, 0.0913, is obtained and compared to analytical data, and shows good agreement. The friction factor for a rod bundle was compared with the Moody correlation for smooth tubes and the Prandtl correlation. The value of the friction factor was lower than the values given by Moody's charts, due to dependency on geometric parameters and the type of spacer grid. The normalized Nusselt number in the rod bundle obtained from the present study is seen to agree well with Yao's correlation. Due to the action of the secondary flow, the normalized Nusselt number was increased abruptly just after the spacer grid. At a distance of $2D_h$ from the beginning of the spacer grids, in the direction of flow, because fluid enthalpy and the Nusselt number have maximum and minimum values, respectively, the

probability of nucleate boiling (DNB) is much higher, and a two phase flow will occur.

REFERENCES

1. Armfield, M.V. "Effects of support grid design on local, single-phase turbulent heat transfer in rod bundles", Master's Thesis, Clemson University (2001).
2. Rehme, K. and Trippe, G. "Pressure drop and velocity distribution in rod bundle with spacer grids", *Nucl. Eng. Des.*, **62**, pp. 349-359 (1980).
3. Sato, Y., Sadatomi, M. and Mine, T. "Flow distribution and pressure drop for parallel flow", *Bulletin of the JSME*, **27**(224), pp. 180-187 (1984).
4. Rehme, K. "The structure of turbulence in rod bundles and the implications of natural mixing between the subchannels", *Int. J. Heat Mass Transfer*, **35**(2), pp. 567-581 (1992).
5. Rehme, K. "The structure of turbulent flow through rod bundles", *Nucl. Eng. Des.*, **99**, pp. 141-154 (1987).
6. Yang, S.K. and Chung, M.K. "Turbulent flow through spacer grids in rod bundles", *Journal of Fluids Engineering*, **120**, pp. 786-791 (1998).
7. Imaizumi, M., Ichioka, T., Hoshi, M., Teshima, H., Kobayashi, H. and Yokoyama, T. "Development of CFD method to evaluate 3-D flow characteristics for PWR fuel assembly", in *Transactions of 13th SMiRT*, Porto Alegre, Brasil (1995).
8. Hoshi, M., Ikeda, K., Izumi, H. and Suemura, T. "Cross flow study of PWR mixed core -evaluation for staggered mixing vane grid", in *Proceedings of ICONE6-6205*, San Diego, USA (1998).
9. Teshima, H., Ikeda, K., Kobayashi, H., Mori, M. and Hoshi, M. "Investigation of PWR fuel rod vibration induced by cross-flow", in *Proceedings of 15th SMiRT*, Seoul, Korea (1999).
10. In, W.K. "Numerical study of coolant mixing caused by the flow deflectors in a nuclear fuel bundle", *Nucl. Technol.*, **134**, pp. 187-195 (2001).
11. Jian, S., Atila, P. and Silva, F. "Analytical prediction of friction factors and Nusselt numbers of turbulent forced convection in rod bundles with smooth and rough surfaces", *Nucl. Eng. Des.*, **215**, pp. 111-127 (2002).
12. Bottcher, M. "Detailed CFX-5 study of the coolant mixing within the reactor pressure vessel of a VVER-1000 reactor during a non-symmetrical heat-up test", *Nucl. Eng. Des.*, **238**(3), pp. 445-452 (2008).
13. Patankar, S.V., *Numerical Heat Transfer and Fluid Flow*, McGraw-Hill, New York (1980).
14. Hughes, W.F. and Gaylord, E.W., *Basic Equations of Engineering Science*, Schaum's Outline Series. McGraw-Hill, New York (1964).
15. Launder, B.E. and Spalding, D.B. "The numerical computation of turbulent flows", *Comput. Meth. Appl. Mech. Eng.*, **3**, pp. 269-289 (1974).
16. Ishigai, S., *Steam Power Engineering: Thermal and Hydraulic Design Principles*, Cambridge University Press (1999).
17. El-Wakil, M.M., *Nuclear Heat Transport*, International Textbook Company (1971).
18. Lee, K.B., Jang, H.C. and Lee, S.K. "Study of the secondary flow effect on the turbulent flow characteristics in fuel rod bundles", *J. Korean Nucl. Soc.*, **26**, pp. 345-354 (1994).
19. Rehme, K. "Pressure drop correlation for fuel element spacers", *Nucl. Technol.*, **17**, pp. 15-23 (1973).
20. White, F.M., *Viscous Fluid Flow*, Third Edition, McGraw-Hill (2006).
21. Welty, J.R., Wilson, R.E. and Wicks, C.E., *Fundamentals of Momentum Heat and Mass Transfer*, 2nd Ed. (1976).
22. Yang, S.K. and Chung, M.K. "Spacer grid effects on turbulent flow in rod bundles", *J. Korean Nucl. Soc.*, **28**, pp. 56-71 (1996a).
23. Rehme, K. "Pressure drop performance of rod bundles in hexagonal arrangements", *Int. J. Heat Mass Transfer*, **15**, pp. 2499-2517 (1972).
24. Incropera, F.P. and Dewitt, D.P., *Heat and Mass Transfer*, 5th Ed., John Wiley and Sons, Inc. (2002).
25. Yao, S.C., Hochreiter, L.E. and Leech, W.J. "Heat-transfer augmentation in rod bundle near grid spacers", *Journal of Heat Transfer*, **104**, pp. 76-81 (1982).

APPENDIX

The axial variation of heat flux along the fuel rod is given by:

$$q'' = q''_c \cos\left(\frac{\pi z}{H}\right), \tag{A1}$$

where q''_c and H are heat flux at the center of the fuel rod and the height of the fuel rod with heat flux, respectively [17]. The value of H in the rod bundle is 3.53 m. The average height of a cosine function, having amplitude of q''_c, is:

$$q''_m = \frac{2}{\pi} q''_c. \tag{A2}$$

The approximate value of the average heat flux in any fuel rod can be obtained by dividing the full power of the reactor per the total surface of the fuel rods [16]:

$$q''_m = \frac{P}{S}. \tag{A3}$$

S is obtained by:

$$S = \pi(163 \times 311)DH, \tag{A4}$$

where D is the diameter of the fuel rod. Now the value of the average of the heat flux in the modeling domain is obtained from:

$$q''_{m,\text{domain}} = \frac{\int_{-\frac{H}{2}}^{-\frac{H}{2}+H_{hf}} q'' dz}{\int_{-\frac{H}{2}}^{-\frac{H}{2}+H_{hf}} dz}, \tag{A5}$$

where H_{hf} is the height of the fuel rod with the heat flux in the modeling domain.

BIOGRAPHY

Bahar Firoozabadi is the associate professor in the school of mechanical engineering at Sharif University of Technology, Tehran. Her research interests are fluid mechanics in density currents; presently focusing on bio fluid mechanics, and porous media. She received her PhD in mechanical engineering also at Sharif University. She teaches fluid mechanics and gas dynamics for undergraduates, and viscous flow, advanced fluid mechanics, continuum mechanics and biofluid mechanics for graduate students.